energies

MDPI

Article

Experimental Study of Hydrogen Combustion and Emissions for a Self-Developed Microturbine

István Péter Kondor

Department of Innovative Vehicles and Materials, University of John von Neumann, Izsáki Str. 10, 6000 Kecskemét, Hungary; kondor.peter@nje.hu

Abstract

This paper presents an experimental investigation of hydrogen enrichment effects on combustion behavior and exhaust emissions in a self-developed micro gas turbine fueled with a propane–butane mixture. Hydrogen was blended with the base fuel in volume fractions of 0–30%, and combustion was examined under unloaded operating conditions at three global equivalence ratios (ϕ = 0.7, 1.1, and 1.3). The global equivalence ratio (ϕ) is defined as the ratio of the actual fuel–air ratio to the corresponding stoichiometric fuel–air ratio, with $\phi < 1$ representing lean, $\phi = 1$ stoichiometric, and $\phi > 1$ fuel-rich operating conditions. The micro gas turbine is based on an automotive turbocharger coupled with a custom-designed counterflow combustion chamber developed specifically for alternative gaseous fuel research. Exhaust gas emissions of CO, CO_2, and NO_x were measured using a laboratory-grade FTIR analyzer (Horiba Mexa FTIR Horiba Ltd., Kyoto, Japan), while combustion chamber temperature was monitored with thermocouples. The results show that hydrogen addition significantly influences flame stability, combustion temperature, and emission characteristics. Increasing the hydrogen fraction led to a pronounced reduction in CO emissions across all equivalence ratios, indicating enhanced oxidation kinetics and improved combustion completeness. CO_2 concentrations decreased monotonically with hydrogen enrichment due to the reduced carbon content of the blended fuel and the shift of combustion products toward higher H_2O fractions. In contrast, NO_x emissions increased with increasing hydrogen content for all tested equivalence ratios, which is attributed to elevated local flame temperatures, enhanced reaction rates, and the formation of locally near-stoichiometric zones in the compact combustor. A slight reduction in NO_x at low hydrogen fractions was observed under near-stoichiometric conditions, suggesting a temporary shift toward a more distributed combustion regime. Overall, the findings demonstrate that hydrogen–propane–butane blends can be stably combusted in a micro gas turbine without major operational issues under unloaded conditions. While hydrogen addition offers clear benefits in terms of CO reduction and carbon-related emissions, effective NO_x mitigation strategies will be essential for future high-hydrogen microturbine applications.

Keywords: hydrogen; microturbine; sustainable fuel; combustion

Check for updates

Academic Editor: Jiaqiang E

Received: 2 January 2026
Revised: 19 January 2026
Accepted: 21 January 2026
Published: 23 January 2026

Copyright: © 2026 by the author. Licensee MDPI, Basel, Switzerland. This article is an open access article distributed under the terms and conditions of the Creative Commons Attribution (CC BY) license.

1. Introduction

Nowadays, efforts to replace fossil fuels have increased significantly not only in the transport sector but also in energy production. A significant part of combined cycle power plants still operate with fossil fuels both in Europe and outside Europe. The operation of high-performance gas turbines using natural gas needs to be replaced in the near future with alternative fuels that meet sustainability requirements. A group of gas turbines used

in energy production are microturbines, which have a power range below 500 kW and are often operated in cogeneration (CHP) or trigeneration (CCHP) systems, where they produce both electricity and heat. Microturbines are basically heat engines operating on the Brayton thermodynamic cycle, which can be operated with or without heat recovery; however, to achieve better efficiency, the heat from the exhaust gas must be partially recovered and used to preheat the turbine air supply before it enters the combustion chamber, using an air-to-air heat exchanger, the so-called recuperator or regenerator. This can increase the efficiency to around 30%, while without heat recovery only 17–20% efficiency can be achieved. As with large gas turbines, the performance of microturbines is determined by the maximum temperature achievable in the combustion chamber, the limits of which are the structural materials used and the heating value of the fuel. Most microturbines allow the use of different fuels. Both liquid and gaseous fuels can be used. In the case of industrial gas turbines and microturbines used today, the most environmentally friendly fuel is natural gas. Its intended use is usually for the generation of electrical power, usually driving permanent magnet variable speed generators that produce a high frequency alternating current which must first be rectified and then converted to alternating current of the appropriate frequency [1–5].

Advantages of micro gas turbines include modularity, low maintenance requirements, air-bearing design, fast start/stop capability, and fuel flexibility. Recent developments increasingly emphasize decarbonization by adapting MGTs to hydrogen, biogas, or hydrogen–hydrocarbon blends. A comprehensive review by Weerakoon et al. (2023) outlines several subfields of MGT research and highlights fuel adaptability as a central trend [6]. Banihabib, R. & Lingstädt, T. et al. (2023) reports on the adaptation of a 100 kW micro gas turbine to run fuel-flexibly (methane/hydrogen blends up to 100 vol.% H_2) [7]. The results include stable operation and NO_x emissions kept below their limits, even at full hydrogen. Cecere et al. (2023) review gas turbine combustion technologies for hydrogen blends up to 100% H_2 and discuss flame stabilization strategies, micro-mixing, exhaust gas recirculation [8]. Aslanidou et al. (2021) outlines that units as small as ~3 kW have been tested with hydrogen/methane blends and that MGTs with hydrogen fuel capability will play an increasing role in distributed generation [9].

2. Materials and Methods

2.1. Structural Elements of the Microturbine

The microturbine consists of an Garrett G40-1150 (Garrett, Rolle, Switzerland) automotive turbocharger and a custom-designed counterflow combustion chamber. A counterflow combustion chamber is a specialized design often used in gas turbines and microturbines, where the hot combustion gases move in the opposite direction of the incoming compressed air. This reversed, "U-shaped" flow path allows the chamber to be more compact and shortens the overall engine length compared to straight-through combustors. Compressed air enters from the rear and travels forward around the combustion liner, with a portion of the air directed through swirlers and openings into the liner for fuel–air mixing. Fuel is injected into the liner and stabilized by swirl vanes or vortex generators, ensuring a steady flame and efficient combustion. At the same time, cooling air flows along the outer liner surface to protect it from excessive temperatures, and dilution holes near the downstream end introduce additional air to lower the temperature before the gases turn back toward the turbine inlet. This counterflow layout not only improves compactness but also enhances thermal management of the casing, since the reversed flow distributes heat more evenly. Effective fuel–air mixing is crucial to avoid hot spots and reduce emissions, and is often supported by staged fuel injection. The design also helps minimize pressure losses compared to longer straight combustors, improving efficiency. However, careful engineering is

required to achieve uniform temperature at the turbine inlet and to withstand high thermal gradients and cyclic loads. Overall, this configuration offers a compact size, effective cooling, and reliable performance, making it a common choice in modern turbine systems. The combustion chamber parameters are shown in Figure 1.

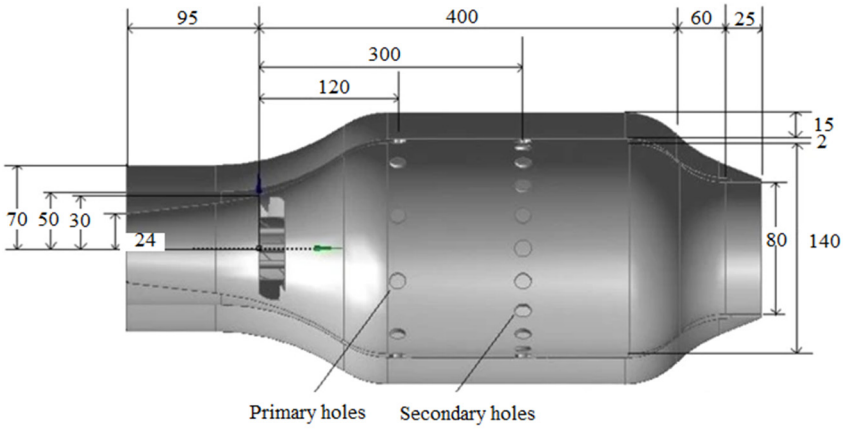


Figure 1. Combustion chamber. The green arrow shows the direction of flow in the combustion chamber. The dashed line shows the imaginary flow channel of the air/fuel mixture from the direction of the air swirlwr element.

The distribution of velocity vectors obtained during simulation tests of the combustion chamber is shown in Figure 2.

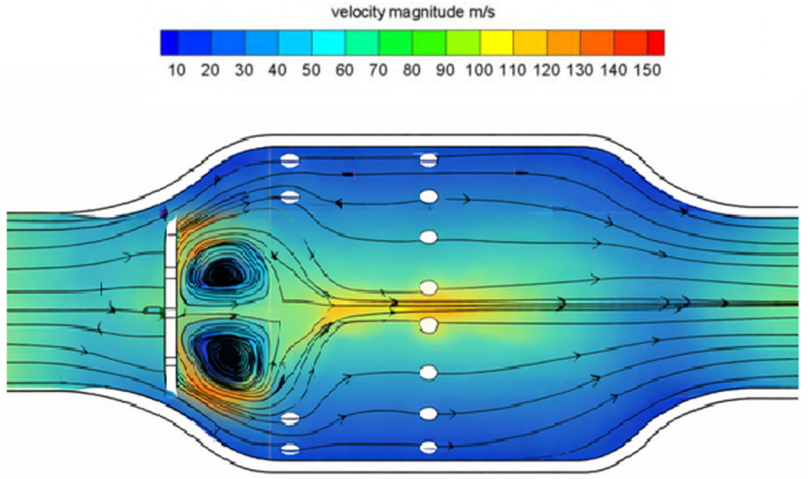


Figure 2. Distribution of velocity vectors. The arrows show the air flow, the holes are the secondary air (cooling air) holes.

The combustion chamber is made of 2 mm-thick stainless KO36Ti plate. The microturbine compressor and turbine unit is powered by a Garrett G40-1150 turbocharger. This is a conventional automotive turbocharger, mainly used for supercharging commercial vehicle engines. The characteristics of the centrifugal compressor are shown in Figure 3.

Additional equipment, such as an ignition system, an oil system for lubricating the supercharger bearings, a filter, and pipelines are also part of the system. The microturbine is started with compressed air fed through the compressor intake duct [10–14].

2.2. Experimental Setup

During the measurements, the microturbine sucked in ambient atmospheric air, which was unconditioned. The amount of air sucked in was controlled by a throttle valve, and an air flow meter was installed after the throttle valve. The control with the throttle valve

was necessary due to the adjustability of the stoichiometric mixing ratio. Temperature measurements were taken at three points: ambient (intake air), combustion chamber, and exhaust gas temperatures. Pressure measurements were taken at the outlet side of the compressor. Emissions were measured with a Horiba Mexa FTIR laboratory emission meter, for which sampling was carried out through the blowpipe with a heated sample line. The fuel was introduced into the combustion chamber through a mixing valve to which a propane–butane and a hydrogen cylinder were connected. The experimental setup is shown in Figure 4.

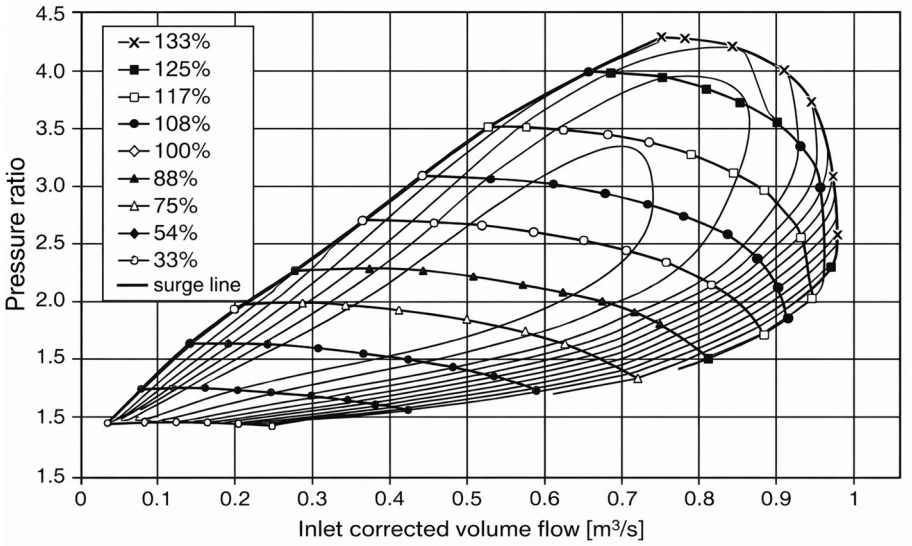


Figure 3. Characteristics of the centrifugal compressor.

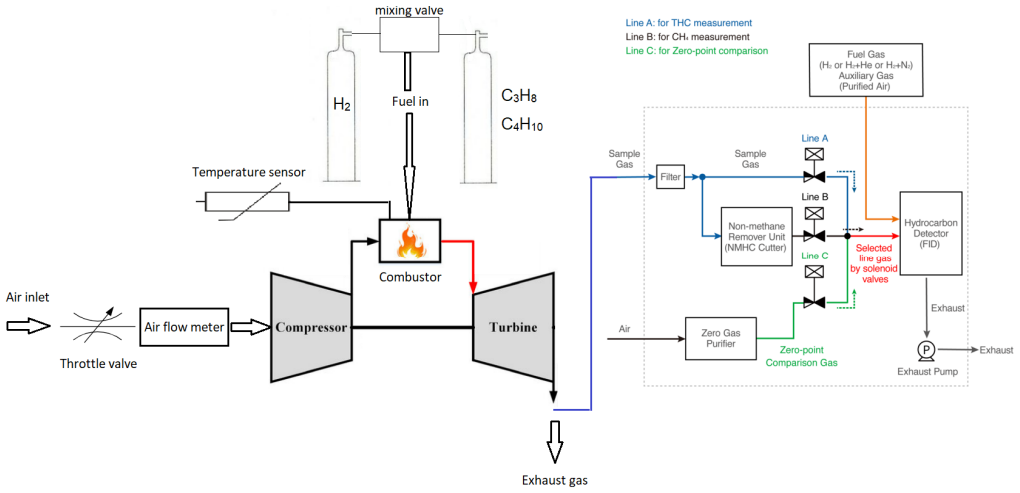


Figure 4. Schematic diagram of the experimental setup. The colors are used to distinguish the paths of different gases and have no significance for interpretation within the emission measurement device.

The equipment used for the measurements is a Fourier Transform Infrared (FTIR) spectrometer, which operates on the principles of absorption and reflection. During the measurement, broadband infrared light passes through the gas sample. The gas molecules absorb radiation at specific frequencies while allowing others to pass. These absorption frequencies correspond to the natural vibrational modes of the molecules or their harmonics. The amount of absorbed light at a given frequency is proportional to the concentration of the gas, which allows both the type of gas and its quantity to be determined from the absorption spectrum. The interferometer modulates the infrared light, effectively separating it into different wavelength components. As the light passes through the measurement

cell, the detector records the intensity of the transmitted radiation. Based on this signal, the electronics calculate the degree of absorption and, using Fourier transformation, convert it into the concentration of the analyzed gases. The accuracy of the measurement instrument summarizes Table 1 [15–18].

Table 1. The accuracy of the measuring instruments.

Measured Component	NO and NO_x	CO	CO_2
Reproducibility (vol.%)	≤0.5% of range full scale	≤0.5% of range full scale	≤0.5% of range full scale
Linearity (vol.%)	≤2% of measured value (10–100% of range full scale) ≤1% of range full scale whichever is smaller	≤2% of measured value (10–100% of range full scale) ≤1% of range full scale whichever is smaller	≤2% of measured value (10–100% of range full scale) ≤1% of range full scale whichever is smaller

2.3. Tested Fuels

Two types of fuels (propane–butane and hydrogen) were tested during the research. Both fuels are commercially available in bottled form. Propane–butane is stored in liquid form and hydrogen is stored in a gaseous state under pressure in standard bottled forms. The properties of the fuels are summarized in Table 2.

Table 2. Properties of propane–butane and hydrogen.

Property/Parameter	Propane 40 vol.%-Butane 60 vol.%	Hydrogen 5.0
Composition	Propane (C_3H_8) 40 vol.% + Butane (C_4H_{10}) 60 vol.%,	Pure molecular hydrogen H_2
Molecular weigh	Propane: 44.10 kg/kmol; Butane: 58.12 kg/kmol	2.016 kg/kmol
Density (gas, at 25 °C, 1 atm)	Propane gas: 1.80 kg/m^3 (≈1.5 × air)	0.0899 kg/m^3 (≈0.07 × air)
Heating value (Higher Heating Value, HHV per mass)	46–50 MJ/kg	141.8 MJ/kg
Autoignition/Ignition temperature	Propane: 470 °C; Butane: 405 °C	500–580 °C
Energy content per volume	25 MJ/L	0.010–0.011 MJ/L
State under storage/transport	Stored/liquefied under pressure, then vaporized for use	Stored under pressure 200 bar (compressed gas)

3. Results and Discussion

The microturbine was tested and adjusted with propane–butane gas. This is the reference fuel to which hydrogen was mixed in various volume percentages during further measurements 5, 10, 20, 30 volumetric %. Each measurement point was measured three times in a steady-state operating condition, with results averaged, over a measurement time of 20 s. During the measurements, the parameters of the ambient air entering the compressor were as follows: air temperature 20 °C, pressure 1015 hPa, and humidity 50%.

3.1. Temperature Conditions

The combustion chamber temperature was measured in the combustion zone with an R-type thermocouple. The diagram below presents the measured combustion temperature values of a micro gas turbine combustor operating with a propane–butane fuel blend and varying hydrogen mixing ratios (0–30 volumetric %) at three different equivalence ratios (φ = 0.7, 1.1, and 1.3). The observed temperature trends can be explained by the combined effects of fuel properties, flame characteristics, and mixture stoichiometry. The combustion chamber temperature at different stoichiometric and mixing ratios is shown in Figure 5.

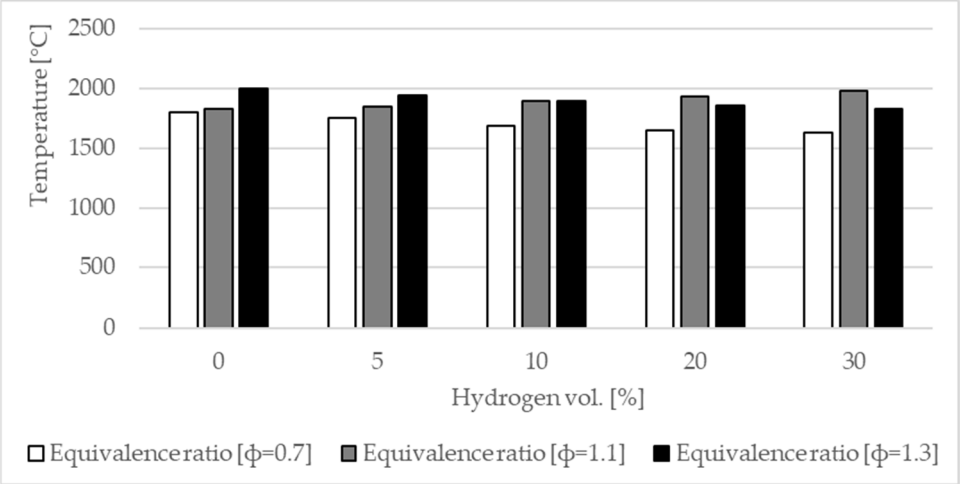


Figure 5. Measured combustion chamber temperature as a function of hydrogen volume fraction at three global equivalence ratios.

At an equivalence ratio of φ = 0.7, the mixture is fuel-lean, meaning that excess air is present in the combustor. As the hydrogen mixing ratio increases, the combustion temperature decreases steadily. This behavior can be attributed to several factors. Although hydrogen has a high laminar flame speed and a high heating value per unit mass, it also has a very low volumetric energy density compared to propane–butane. When hydrogen replaces part of the hydrocarbon fuel, the total chemical energy released per unit volume of the fuel–air mixture decreases. In a lean regime, the excess air further dilutes the flame, increasing heat losses and reducing adiabatic flame temperature. Additionally, hydrogen-enriched lean flames tend to have higher specific heat losses due to increased water vapor formation, which absorbs part of the released energy. As a result, the overall combustion temperature decreases with increasing hydrogen content.

At φ = 1.1, the mixture is slightly fuel-rich and closer to stoichiometric conditions. In this regime, the combustion temperature increases with increasing hydrogen fraction. Here, hydrogen addition improves combustion efficiency. Hydrogen's high flame speed enhances flame stability and promotes a more complete oxidation of the fuel mixture. This reduces incomplete combustion losses that are more pronounced with pure propane–butane. Moreover, near-stoichiometric conditions allow the chemical energy of hydrogen to be more effectively converted into thermal energy, leading to a higher flame temperature. The increased reaction rates and improved heat release outweigh the dilution effect observed under lean conditions.

At φ = 1.3, the mixture is significantly fuel-rich. In this case, increasing the hydrogen content leads to a gradual decrease in combustion temperature. Under rich conditions, oxygen availability becomes the limiting factor. Although hydrogen reacts rapidly, the lack of sufficient oxidizer prevents complete combustion. The addition of hydrogen displaces part of the propane–butane fuel but does not compensate for the reduced oxygen availability. This results in incomplete oxidation and lower effective heat release. Furthermore, rich combustion increases radiative and dissociation losses, which also contribute to the observed temperature reduction [19–21].

3.2. Emission Results

Hydrogen affects the composition of harmful substances in exhaust gas. It changes the chemical composition of the emission parameters being tested. Three pollutant components were measured from the sample taken from the exhaust gases: CO, CO_2, and NO_x. For all

three components, the emission values were tested at three stoichiometric ratios of ϕ = 0.7, ϕ = 1, and ϕ = 1.3.

3.2.1. CO Emission

At φ = 0.7 (lean mixture), the mixture contains an overall excess of oxygen, so in an ideal, perfectly hot, perfectly mixed system, we would expect low CO levels. However, in real microturbines, lean operation often results in high CO levels because CO oxidation is limited by temperature and kinetics: lean flames have lower adiabatic flame temperatures. The gases after the flame cool rapidly due to dilution and wall heat loss. CO oxidation can "freeze out" if the temperature falls below the range where CO → CO_2 can occur quickly enough.

This explains why the lean baseline (0% H_2) contains the highest CO (2690 ppm). It also explains why H_2 blending helps the lean case so much: the system is not oxygen-limited; it is reaction-rate-limited. H_2 directly addresses this by improving stability and the OH radical pool, so CO falls strongly (to 1210 ppm at 30% H_2) [22]. The evolution of CO as a function of the addition of hydrogen at different stoichiometric mixing ratios is shown in Figure 6.

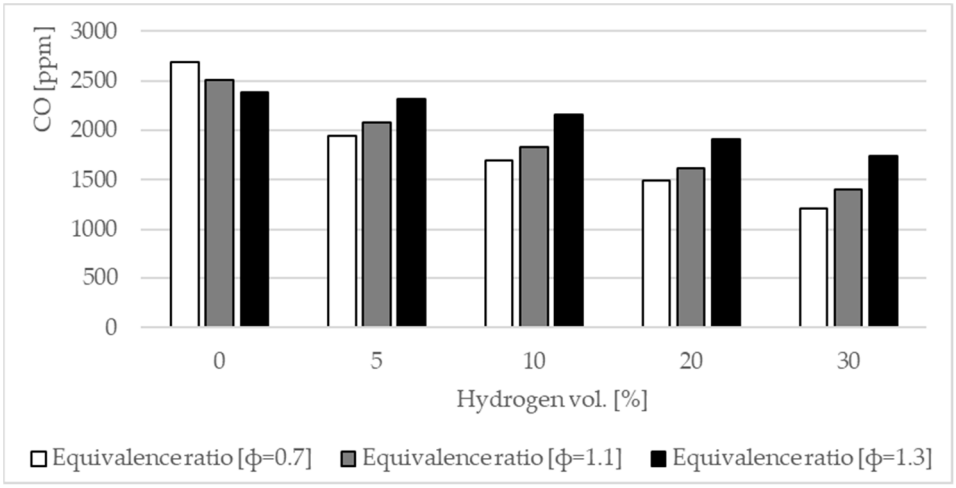


Figure 6. CO emission at different stoichiometric values and hydrogen concentrations.

At φ > 1, oxygen limitation can increase CO in principle, but H_2 blending still helps through carbon displacement (less C → less CO formation potential), better flameholding and fewer partially reacting pockets, faster hydrocarbon breakdown and more robust oxidation chemistry, and possible shifts in local mixing patterns (H_2 jets diffuse faster, which can reduce rich pockets that are strong CO sources).

The relative reduction with H_2 is smaller at a concentration of φ = 0.7 than at φ = 0.7. As the mixture becomes richer, CO can be increasingly influenced by the local O_2 availability, which H_2 cannot fully compensate for [23].

3.2.2. CO_2 Emission

CO_2 is a natural end product of the complete combustion of fuel and air, which is formed when the carbon in the fuel reacts with the oxygen in the air during the combustion process. Hydrogen does not contain carbon, so if part of the hydrocarbon fuel is replaced with H_2, the effective H/C ratio of the mixture increases and the amount of carbon per unit of energy released decreases. For the same turbine power (or the same total fuel energy input), the combustion chamber produces less CO_2 because fewer carbon atoms are burned. This effect alone can explain the consistent downward trend observed for all φ values (e.g., φ = 0.7: 40,520 → 36,420 ppm, which is a decrease of about ~10%).

The exhaust gas composition shifts towards more H_2O and less CO_2. Hydrogen addition increases H_2O formation relative to CO_2 formation. If CO_2 is reported on a wet basis, a higher water vapor fraction directly reduces the CO_2 volume fraction (dilution by H_2O). If CO_2 is reported on a dry basis, this specific "water dilution" is mostly removed—but the carbon removal effect still remains and dominates. Microturbines often run with substantial excess air and can change compressor operating point, bleed flows, or dilution flows. If the system at $\varphi = 0.7$ is operating with a different dilution/recirculation pattern than at $\varphi = 1.1$, the resulting exhaust CO_2 ppm can be higher even if fuel flow is lower. If values are corrected to a reference O_2 level (common in emissions practice), lean cases can shift upward after correction. Very lean mixtures can lower flame temperature and slow oxidation, sometimes increasing CO and UHC at the expense of complete CO_2 formation. Around slightly rich operation, two competing effects occur: Less excess air means less dilution, which would raise CO_2 concentration. But oxygen becomes limited enough that some carbon is diverted into CO and unburned hydrocarbons, which would lower CO_2 formation. At $\varphi = 1.3$ there is less air (and thus less N_2 ballast) per unit fuel, so even if a smaller fraction of carbon reaches CO_2, the exhaust total molar flow is lower, and the CO_2 that is formed can occupy a larger volume fraction. Also, richer operation can change combustor aerodynamics (primary/secondary zone split, liner cooling/dilution mixing), which strongly affects the final measured concentration at the sampling point. Overall, the monotonic drop in CO_2 ppm with increasing hydrogen fraction is most straightforwardly explained by the reduced carbon content of the blended fuel (hydrogen contains no carbon), plus a shift in combustion products toward more H_2O. Differences between $\varphi = 0.7$, 1.1, and 1.3 are likely driven by a balance between carbon oxidation completeness (CO/UHC formation under richer or colder/leaner conditions) and, critically, dilution effects: the total exhaust molar flow and mixing (excess air and N_2 ballast) can change enough that CO_2 concentration in ppm does not track fuel flow in a simple linear way. In the data, $\varphi = 1.1$ appears to fall in a regime where the combined effects yield the lowest measured CO_2 concentration, while $\varphi = 1.3$ shows higher CO_2 ppm again because reduced air dilution can outweigh reduced conversion to CO_2. The FTIR analyzer measures CO_2 concentration on a wet basis (including water vapor) but calculates dry basis concentrations [24]. The evolution of carbon dioxide with the addition of hydrogen at different stoichiometric ratios is shown in Figure 7.

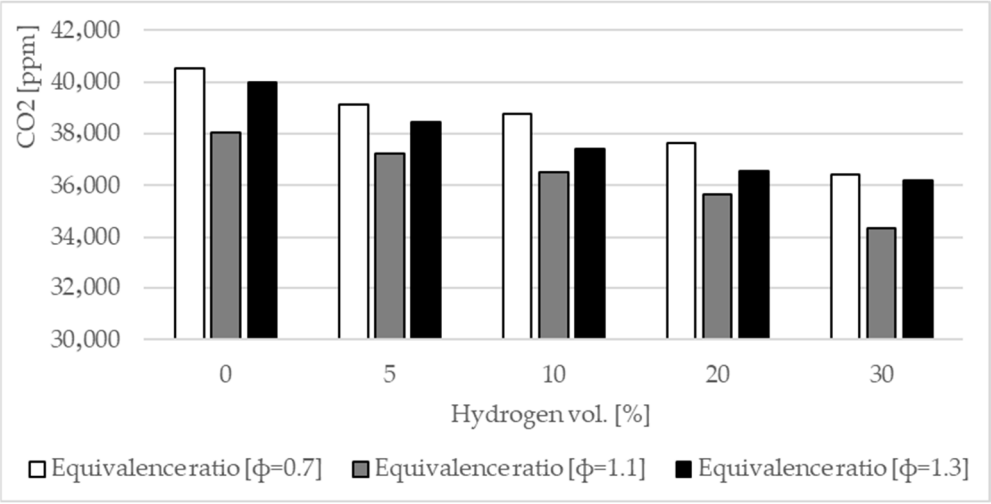


Figure 7. CO_2 emission at different stoichiometric values and hydrogen concentrations.

3.2.3. NO_x Emission

Lean operation generally reduces NO_x as the average flame temperature decreases with excess air. However, lean data increases from 22,450→26,380 ppm with increasing H_2. A lean flame can increase the effective residence time of gases in the hot zone and increase local peak temperatures. It reduces local flame quenching so that fewer cold zones interrupt the high-temperature zone. In a small, highly preheated combustion chamber, even a lean flame can maintain very hot cores if the flame becomes more compact. It creates locally stoichiometric regions due to mixture stratification. Even with a global $\phi = 0.7$, if some regions locally approach $\phi \approx 1$, thermal NO_x increases disproportionately. Thus, the lean mixture trend can be explained by local peak temperature and flame structure effects, which dominate over the global lean mixture temperature decrease.

For $\phi = 1.1$ 25,010 → 24,200 (at 5% H_2) → 27,100 → 28,250 → 29,310; a small initial H_2 addition can reduce NO_x by improving the aerodynamic/chemical balance of the combustion chamber in a way that reduces the peak temperature. For example, more distributed combustion: a small amount of H_2 can broaden the stable operating range and allow the flame to stabilize in a slightly more premixed or distributed mode, reducing the intensity of hot spots. Flame position shift: a small amount of H_2 can move the flame away from the hottest recirculation core or reduce wall/recirculation interactions that create localized high temperature zones. Variations in equivalence ratio control artifacts: in real microturbines, the "same ϕ" in the table may not be exactly the same as the true local ϕ if fueling is based on volume, mass, or LHV/Wobbe index assumptions. A small mixture can briefly lean the actual operating point slightly (or increase effective dilution), reducing NO_x emissions before the additional H_2 drives up the temperature and kinetics.

Rich flames typically have less oxygen available, so lower thermal NO_x levels can be expected. In fact, the baseline at 0% H_2 is the lowest (21,805 ppm). But then NO_x increases to 26,998 ppm at 30% H_2. Rich flames are very sensitive to mixing: even in a globally rich combustion chamber, there can be local near-stoichiometric zones where air and fuel mix well (shear layers, recirculation edges). H_2 can enhance combustion in these zones (faster kinetics), making them hotter and more NO_x-producing. Additionally, there can be a higher local flame temperature despite global richness: Adding H_2 can reduce the soot/radiation losses typical of richer hydrocarbon flames. Less radiative heat loss can raise local temperatures and increase thermal NO_x levels. Most NO is formed in the combustor and may partially oxidize to NO_2 downstream. The higher heating value of hydrogen increases the temperature in the combustion chamber at a rate proportional to the degree of mixing, thus favoring the formation of nitrogen oxides. There are several solutions for reducing NO_x in gas turbines, which can reduce the level of emissions such as Lean Premixed Combustion Dry Low NO_x (DLN)/Dry Low Emission (DLE), or Secondary (post-combustion) method Selective Catalytic Reduction (SCR) [25]. The evolution of NO_x with the addition of hydrogen at different stoichiometric ratios is shown in Figure 8.

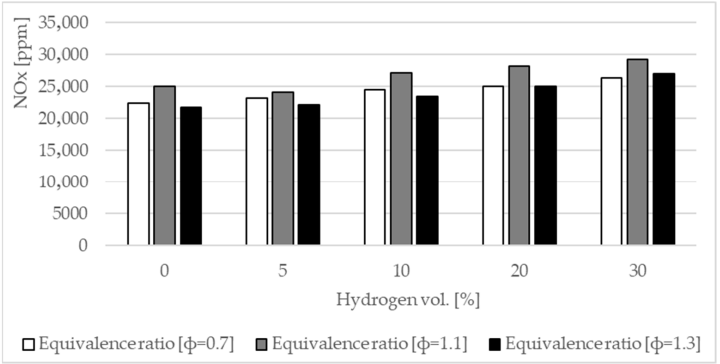


Figure 8. NO_x emission at different stoichiometric values and hydrogen concentrations.

Essentially, the combustion chamber temperature increases under load, but in the case of lean mixture combustion chambers, the rate of increase is not linear at the measured flame peak temperature.

4. Conclusions

This study investigated the feasibility of hydrogen enrichment in a propane–butane-fueled micro gas turbine combustor under unloaded operating conditions. Hydrogen was added in volume fractions of 5, 10, 20, and 30% at three global equivalence ratios (ϕ = 0.7, 1.1, and 1.3). The discussion below synthesizes the observed temperature and emission trends and places them in the context of hydrogen combustion characteristics and microturbine operation. The experimental results clearly show that hydrogen addition significantly alters the combustion behavior inside the compact counterflow combustor. The influence of hydrogen on combustion temperature strongly depends on the equivalence ratio. Under near-stoichiometric conditions ($\phi \approx 1.1$), hydrogen enrichment led to an increase in combustion chamber temperature. This effect is not solely related to the heating value of hydrogen, but primarily to its high laminar flame speed, enhanced chemical reactivity, and improved flame stabilization. These properties promote faster heat release and reduce incomplete combustion zones, resulting in higher local flame temperatures. In contrast, under lean (ϕ = 0.7) and rich (ϕ = 1.3) conditions, increasing hydrogen content resulted in a decrease in measured combustion temperature. In lean operation, excess air and increased water vapor formation enhance thermal dilution and heat losses, while in rich operation, oxygen availability limits complete oxidation, reducing effective heat release despite faster hydrogen kinetics. Hydrogen enrichment had a consistently beneficial effect on CO emissions across all equivalence ratios. The pronounced reduction in CO, particularly under lean conditions, indicates that hydrogen effectively accelerates oxidation chemistry by increasing the availability of reactive radicals (especially OH) and stabilizing the flame. In lean microturbine combustion, CO emissions are often governed by kinetic limitations rather than oxygen availability. Hydrogen addition mitigates this limitation, enabling more complete oxidation before exhaust gases cool and reactions freeze out. Even under rich conditions, where oxygen becomes limiting, hydrogen reduced CO emissions by displacing carbon-containing fuel and improving local mixing, although the relative reduction was smaller than in the lean case.

The observed decrease in CO_2 concentration with increasing hydrogen fraction is primarily attributed to the reduced carbon content of the blended fuel. Since hydrogen contains no carbon, replacing part of the propane–butane fuel lowers the amount of carbon oxidized per unit of released energy. Consequently, the exhaust gas composition shifts toward higher H_2O and lower CO_2 fractions. Secondary effects, such as dilution by excess air and changes in exhaust molar flow, also influence the absolute CO_2 concentrations and explain the differences observed between equivalence ratios. Nevertheless, the monotonic decrease in CO_2 with increasing hydrogen content is consistent with fundamental combustion stoichiometry and confirms the carbon-reduction potential of hydrogen blending.

In contrast to CO and CO_2, NO_x emissions increased with increasing hydrogen content for all tested equivalence ratios, although a slight reduction was observed at low hydrogen fractions near stoichiometric conditions. The overall increase in NO_x can be explained by higher local flame temperatures, intensified reaction rates, and the formation of local near-stoichiometric zones within the combustor. Even under globally lean or rich conditions, hydrogen-enhanced flames tend to be more compact and stable, which increases peak temperatures and residence times in high-temperature regions, favoring thermal NO_x formation. The small NO_x reduction observed at low hydrogen addition under near-stoichiometric conditions likely reflects a temporary shift toward a more dis-

tributed combustion regime or subtle changes in flame position and mixing that reduce peak temperature intensity. However, as hydrogen content increases further, the dominant effect becomes enhanced thermal NO_x formation [26–33].

Overall, the results demonstrate that hydrogen–propane–butane blends can be stably combusted in a self-developed micro gas turbine without operational instabilities under unloaded conditions. Hydrogen addition provides clear advantages in terms of CO reduction and lower carbon-related emissions, confirming its potential as a transitional fuel for decarbonizing microturbine-based energy systems. However, the accompanying increase in NO_x highlights the necessity of appropriate mitigation strategies, such as lean premixed combustion concepts or post-combustion control technologies (e.g., SCR), particularly for higher hydrogen fractions. Future work should focus on loaded operation, the influence of recuperation, and advanced combustor design solutions to fully exploit the benefits of hydrogen while maintaining acceptable NO_x emission levels.

Unlike many previous studies that rely on commercial microturbines or numerical models, this work presents experimental results obtained on a self-developed micro gas turbine based on an automotive turbocharger and a custom-designed counterflow combustion chamber. This configuration represents a research-oriented platform with significantly different geometric constraints, residence times, and mixing characteristics compared to industrial-scale or commercial systems. As a result, the observed combustion and emission behavior cannot be directly extrapolated from larger gas turbines or standardized microturbine units.

Funding: This research received no external funding.

Data Availability Statement: The raw data supporting the conclusions of this article will be made available by the authors on request.

Conflicts of Interest: The author declares no conflict of interest.

Abbreviations

CO	Carbon Monoxide
CO_2	Carbon Dioxide
C_3H_8	Propane
C_4H_{10}	Butane
DLE	Dry Low Emission
NO_x	Nitrogen Oxides
FTIR	Fourier Transform Infrared Detector
H_2	Hydrogen
H_2O	Water
hPa	Hectopascal
kW	Kilowatt
LHV	Lower Heating Value
CHP	Combined Heat and Power
CCHP	Combined Cooling, Heating and Power
MGT	Micro Gas Turbine
MJ	Megajoule
UHC	Unburned Hydrocarbons
SCR	Selective Catalytic Reduction
ϕ	Equivalence ratio

References

1. Przysowa, R.; Gawron, B.; Białecki, T.; Łęgowik, A.; Merkisz, J.; Jasiński, R. Performance and Emissions of a Microturbine and Turbofan Powered by Alternative Fuels. *Aerospace* **2021**, *8*, 25. [CrossRef]
2. Hack, R.L.; McDonell, V.G. Impact of Ethane, Propane, and Diluent Content in Natural Gas on the Performance of a Commercial Microturbine Generator. *ASME. J. Eng. Gas Turbines Power* **2008**, *130*, 011509. [CrossRef]
3. Sakurai, T.; Yuasa, S.; Ono, Y.; Honda, T. Flame stability and emission characteristics of propane-fueled flat-flame miniature combustor for ultra-micro gas turbines. *Combust. Flame* **2013**, *160*, 2497–2506. [CrossRef]
4. Nozari, M.; Eidiattarzade, M.; Tabejamaat, S.; Kankashvar, B. Emission and performance of a micro gas turbine combustor fueled with ammonia-natural gas. *Int. J. Engine Res.* **2021**, *23*, 1012–1026. [CrossRef]
5. Capata, R.; Saracchini, M. Experimental Campaign Tests on Ultra Micro Gas Turbines, Fuel Supply Comparison and Optimization. *Energies* **2018**, *11*, 799. [CrossRef]
6. Weerakoon, A.S.; Assadi, M. Trends and advances in micro gas turbine technology for sustainable energy solutions: A detailed review. *Energy Convers. Manag. X* **2023**, *20*, 100483. [CrossRef]
7. Banihabib, R.; Lingstädt, T.; Wersland, M.; Kutne, P.; Assadi, M. Development and testing of a 100 kW fuel-flexible micro gas turbine running on 100% hydrogen. *Int. J. Hydrogen Energy* **2024**, *49*, 92–111. [CrossRef]
8. Cecere, D.; Giacomazzi, E.; Di Nardo, A.; Calchetti, G. Gas Turbine Combustion Technologies for Hydrogen Blends. *Energies* **2023**, *16*, 6829. [CrossRef]
9. Aslanidou, I.; Rahman, M.; Zaccaria, V.; Kyprianidis, K.G. Micro Gas Turbines in the Future Smart Energy System: Fleet Monitoring, Diagnostics, and System Level Requirements. *Front. Mech. Eng.* **2021**, *7*, 676853. [CrossRef]
10. Sircilli, F.; Retief, S.J.; Magalhães, L.B.; Ribeiro, L.R.; Zanandrea, A.; Brink, C.; Nascimento, M.; Dreyer, M.M. Measurements of a micro gas turbine plume and data reduction for the purpose of infrared signature modeling. *IEEE Trans. Aerosp. Electron. Syst.* **2016**, *51*, 3282–3293. [CrossRef]
11. Enagi, I.I.; Al-Attab, K.; Zainal, Z. Combustion chamber design and performance for micro gas turbine application. *Fuel Process. Technol.* **2017**, *166*, 258–268. [CrossRef]
12. Nikpey, H.; Assadi, M.; Breuhaus, P.; Mørkved, P. Experimental evaluation and ANN modeling of a recuperative micro gas turbine burning mixtures of natural gas and biogas. *Appl. Energy* **2014**, *117*, 30–41. [CrossRef]
13. Giacomazzi, E.; Troiani, G.; Di Nardo, A.; Calchetti, G.; Cecere, D.; Messina, G.; Carpenella, S. Hydrogen Combustion: Features and Barriers to Its Exploitation in the Energy Transition. *Energies* **2023**, *16*, 7174. [CrossRef]
14. Nemitallah, M.A.; Abdelhafez, A.A.; Habib, M.A. Gas Turbine Performance for Different Burner Technologies. In *Approaches for Clean Combustion in Gas Turbines. Fluid Mechanics and Its Applications*; Springer: Cham, Switzerland, 2020; Volume 122. [CrossRef]
15. Arenas-Fernández, A.; Rodríguez-de Arriba, P.; Escamilla-Perejón, A.; González-Almenara, R.; Sánchez, D. Using Hydrogen for the Generation of Non-Propulsive Energy in Civil Aviation-Design and Performance of Combined Micro Gas Turbine and Organic Rankine Cycle Systems. In *Proceedings of the ASME Turbo Expo 2024: Turbomachinery Technical Conference and Exposition. Volume 5: Cycle Innovations, London, UK, 24–28 June 2024*; V005T06A036; ASME: New York, NY, USA, 2024. [CrossRef]
16. Colorado, A.; McDonell, V. Reactor Network Analysis to Assess Fuel Composition Effects on NOx Emissions From a Recuperated Gas Turbine. In *Proceedings of the ASME Turbo Expo 2014: Turbine Technical Conference and Exposition. Volume 4B: Combustion, Fuels and Emissions, Düsseldorf, Germany, 16–20 June 2014*; V04BT04A030; ASME: New York, NY, USA, 2014. [CrossRef]
17. Alnaeli, M.; Alnajideen, M.; Navaratne, R.; Shi, H.; Czyzewski, P.; Wang, P.; Eckart, S.; Alsaegh, A.; Alnasif, A.; Mashruk, S.; et al. High-Temperature Materials for Complex Components in Ammonia/Hydrogen Gas Turbines: A Critical Review. *Energies* **2023**, *16*, 6973. [CrossRef]
18. Pashchenko, D. Hydrogen-rich gas as a fuel for the gas turbines: A pathway to lower CO_2 emission. *Renew. Sustain. Energy Rev.* **2023**, *173*, 113117. [CrossRef]
19. Li, F.; Liu, D.; Sun, K.; Yang, S.; Peng, F.; Zhang, K.; Guo, G.; Si, Y. Towards a Future Hydrogen Supply Chain: A Review of Technologies and Challenges. *Sustainability* **2024**, *16*, 1890. [CrossRef]
20. Kang, Z.; Shi, Z.; Ye, J.; Tian, X.; Huang, Z.; Wang, H.; Wei, D.; Peng, Q.; Tu, Y. A Review of Micro Power System and Micro Combustion: Present Situation, Techniques and Prospects. *Energies* **2023**, *16*, 3201. [CrossRef]
21. Villatoro, W.; McDonell, V.; Hu, R.; Ayers, D. Evaluation of the Performance of a 200 kW Recuperated Gas Turbine Engine Operated on Up to 30% Hydrogen Added to Natural Gas. In *Proceedings of the ASME Turbo Expo 2022: Turbomachinery Technical Conference and Exposition. Volume 3A: Combustion, Fuels, and Emissions, Rotterdam, The Netherlands, 13–17 June 2022*; V03AT04A042; ASME: New York, NY, USA, 2022. [CrossRef]
22. Asti, A.; Stewart, J.F.; Forte, A.; Yilmaz, E.; D'Ercole, M. Enlarging the Fuel Flexibility Boundaries: Theoretical and Experimental Application to a New Heavy-Duty Gas Turbine (MS5002E). In *Proceedings of the ASME Turbo Expo 2008: Power for Land, Sea, and Air. Volume 3: Combustion, Fuels and Emissions, Parts A and B, Berlin, Germany, 9–13 June 2008*; ASME: New York, NY, USA, 2008; pp. 553–563. [CrossRef]

23. Wang, Y.; Sohn, C.H.; Kim, J.-Y. Effects of hydrogen blending on combustion and pollutant emission of propane/air in a model furnace with a rotary kiln burner. *Therm. Sci. Eng. Prog.* **2024**, *47*, 102330. [CrossRef]
24. Cellek, M.S.; Pınarbaşı, A. Investigations on performance and emission characteristics of an industrial low swirl burner while burning natural gas, methane, hydrogen-enriched natural gas and hydrogen as fuels. *Int. J. Hydrogen Energy* **2018**, *43*, 1194–1207. [CrossRef]
25. Öztürk, A.T.; Akal, D.; Akyol, U. Investigation of the emission values of butane, methane and methane-hydrogen mixtures used in household stove burners. *Int. J. Hydrogen Energy* **2025**, *141*, 88–98. [CrossRef]
26. Sekar, M.; Alahmadi, T.A.; Nithya, S. Numerical simulation of industrial gas burners fueled with hydrogen-methane mixtures for enhanced combustion efficiency and reduced greenhouse gas emissions. *Fuel* **2024**, *370*, 131807. [CrossRef]
27. Büyükakın, M.K.; Öztuna, S. Numerical investigation on hydrogen-enriched methane combustion in a domestic back-pressure boiler and non-premixed burner system from flame structure and pollutants aspect. *Int. J. Hydrogen Energy* **2020**, *45*, 35246–35256. [CrossRef]
28. Franco, A.; Rocca, M. Industrial Decarbonization through Blended Combustion of Natural Gas and Hydrogen. *Hydrogen* **2024**, *5*, 519–539. [CrossRef]
29. Alhuyi Nazari, M.; Fahim Alavi, M.; Salem, M.; Assad, M.E.H. Utilization of hydrogen in gas turbines: A comprehensive review. *Int. J. Low-Carbon Technol.* **2022**, *17*, 513–519. [CrossRef]
30. Montoya, J.P.G.; Amell, A.A.; Olsen, D.B. Prediction and measurement of the critical compression ratio and methane number for blends of biogas with methane, propane and hydrogen. *Fuel* **2016**, *186*, 168–175. [CrossRef]
31. Zhen, H.; Cheung, C.; Leung, C.; Choy, Y. Effects of hydrogen concentration on the emission and heat transfer of a premixed LPG-hydrogen flame. *Int. J. Hydrogen Energy* **2012**, *37*, 6097–6105. [CrossRef]
32. Miao, J.; Leung, C.; Huang, Z.; Cheung, C.; Yu, H.; Xie, Y. Laminar burning velocities, Markstein lengths, and flame thickness of liquefied petroleum gas with hydrogen enrichment. *Int. J. Hydrogen Energy* **2014**, *39*, 13020–13030. [CrossRef]
33. Kondor, I.P. Sustainable Fuels for Gas Turbines—A Review. *Sustainability* **2025**, *17*, 6166. [CrossRef]

Disclaimer/Publisher's Note: The statements, opinions and data contained in all publications are solely those of the individual author(s) and contributor(s) and not of MDPI and/or the editor(s). MDPI and/or the editor(s) disclaim responsibility for any injury to people or property resulting from any ideas, methods, instructions or products referred to in the content.